PB 161590

NBS

Technical Note 89

COLLISIONS OF LIQUID DROPS WITH LIQUIDS

U. S. DEPARTMENT OF COMMERCE
NATIONAL BUREAU OF STANDARDS

THE NATIONAL BUREAU OF STANDARDS

Functions and Activities

The functions of the National Bureau of Standards are set forth in the Act of Congress, March 3, 1901, as amended by Congress in Public Law 619, 1950. These include the development and maintenance of the national standards of measurement and the provision of means and methods for making measurements consistent with these standards; the determination of physical constants and properties of materials; the development of methods and instruments for testing materials, devices, and structures; advisory services to government agencies on scientific and technical problems; invention and development of devices to serve special needs of the Government; and the development of standard practices, codes, and specifications. The work includes basic and applied research, development, engineering, instrumentation, testing, evaluation, calibration services, and various consultation and information services. Research projects are also performed for other government agencies when the work relates to and supplements the basic program of the Bureau or when the Bureau's unique competence is required. The scope of activities is suggested by the listing of divisions and sections on the inside of the back cover.

Publications

The results of the Bureau's work take the form of either actual equipment and devices or published papers. These papers appear either in the Bureau's own series of publications or in the journals of professional and scientific societies. The Bureau itself publishes three periodicals available from the Government Printing Office: The Journal of Research, published in four separate sections, presents complete scientific and technical papers; the Technical News Bulletin presents summary and preliminary reports on work in progress; and Basic Radio Propagation Predictions provides data for determining the best frequencies to use for radio communications throughout the world. There are also five series of nonperiodical publications: Monographs, Applied Mathematics Series, Handbooks, Miscellaneous Publications, and Technical Notes.

Information on the Bureau's publications can be found in NBS Circular 460, Publications of the National Bureau of Standards ($1.25) and its Supplement ($1.50), available from the Superintendent of Documents, Government Printing Office, Washington 25, D.C.

NATIONAL BUREAU OF STANDARDS

Technical Note

89

MAY 1961

COLLISIONS OF LIQUID DROPS WITH LIQUIDS

Olive G. Engel

NBS Technical Notes are designed to supplement the Bureau's regular publications program. They provide a means for making available scientific data that are of transient or limited interest. Technical Notes may be listed or referred to in the open literature. They are for sale by the Office of Technical Services, U. S. Department of Commerce, Washington 25, D. C.

DISTRIBUTED BY

UNITED STATES DEPARTMENT OF COMMERCE

OFFICE OF TECHNICAL SERVICES

WASHINGTON 25, D. C.

Price $1.00

CONTENTS

COLLISIONS OF LIQUID DROPS WITH LIQUIDS*

by

Olive G. Engel

ABSTRACT

The information available on collisions of liquid drops with liquids is reviewed. Measurements of the depth and diameter of the cavity produced in the target liquid made on G. J. Franz's high-speed motion pictures of collisions of waterdrops with water are reported. The measurement data are considered to be of a preliminary nature. The most important provisional observations drawn from them are: the cavity depth-versus-time curve is a parabola or ellipse tangent to the depth axis at the origin; the depth/diameter ratio of the cavity varies with time elapsed since the collision and has a value of 0.5 at only two points in time. An equation for maximum cavity depth is derived on the basis of the three assumptions that the impinging drop is spherical, that the cavity is hemispherical, and that the volume of the cavity is proportional to the kinetic energy of the drop. Test of the equation with the measurement data indicates that the assumptions are reasonably good in the low free-fall velocity range. Apparatus that is now being assembled at the National Bureau of Standards to obtain more accurate data and to carry out an exhaustive study of this type of collision is described.

---

*This NBS Technical Note is based on a report entitled "Collisions of Liquid Drops with Liquids. Part I. A Review with Some Preliminary Data", dated June 1960, covering work performed as part of a project sponsored by the Nonmetallic Materials Laboratory, Materials Central, Wright Air Development Division, Air Research and Development Command, United States Air Force. Since this technical report was submitted, A. C. Charters of the National Aeronautics and Space Administration has published in the October 1960 issue of Scientific American a popularized discussion of some of the fluid-impact phenomena that have been examined quantitatively herein.

1. INTRODUCTION

Collisions between liquid drops and liquids have become important in the present era of space flight. This is not only because of the possibility of collisions between space craft and meteors but also because of the possibility of collisions between themelted leading surface of a re-entering space vehicle and waterdrops in the atmosphere.

Meteors travel at velocities of from 12 to 72 km/sec (39,000 to 240,000 ft/sec). On the basis of the argument that the aerodynamic ($1/2\rho V^2$) pressure at the penetration of a meteor into rock is more than 1,000 times the plastic limit of steel, Öpik [1][a] has suggested that meteor impact, at least in its initial stages, is the case of the impact of a liquid drop of density δ into a liquid medium of density ρ. It appears, however, that concomitant vaporization, and possibly explosion, of the projectile and eventually of the target may complicate the simple liquid-drop-into-liquid picture [2, 3].

With regard to collisions between waterdrops in the atmosphere and the melted leading surface of a space vehicle, it has been recommended [4] that hypervelocity collisions between waterdrops and melting aerodynamic surfaces should be studied. It is very difficult to study high-speed collisions between a liquid projectile and a liquid target because of the problems involved in accelerating liquids. It appears, however, that a study of free-fall-velocity collisions of this kind may produce information of value for the high-velocity case because the Reynolds Number at free-fall velocity is high enough that there should be both dynamical and geometrical similarity.

1.1 Previous Investigations

Even in the free-fall velocity range, only the qualitative aspects of this type of collision have been studied. No equation appears to exist that gives crater depth as a function of collision velocity; no measurements of the depth and diameter of craters produced at different velocities appear to have been made.

Worthington [5, 6, 7] made a study of collisions of liquid drops with liquids with use of an approximately 3-μ sec spark that could be timed to illuminate any stage of the collision repeatedly within a

---

[a] Numbers in brackets refer to literature references at the end of this paper.

time range of a few millisec (msec). In his first study [5], after a sufficient number of observations of a given stage had been made to secure accuracy, he made a sketch of the configuration of that stage. In a later study [6], the sketches were replaced by spark photographs.

High-speed pictures of this type of collision have also been given by Edgerton and Killian [8] in their book on ultra high-speed photography, and by Franz [9] who took high-speed motion pictures of waterdrops falling into water.

The specific liquid-projectile liquid-target combinations that have been studied are: milk drops falling into water [5, 6, 7], milk drops falling into olive oil [5], waterdrops falling into milk mixed with water [6, 7], milk drops falling into milk [8], and waterdrops falling into water [7, 9]. The stages of the collision for all of these liquid-projectile liquid-target combinations are similar; the degree to which a given stage progresses, however, appears to depend on the properties of the liquids involved and on the mass and velocity of the colliding drop.

1.2 Description of the Collision Event

The collision event, as it occurs under various sets of conditions, has been described in the literature and some information on the time required for the successive stages to take place has been obtained 5, 6, 7, 8, 9]. A general description of the major stages is given below for a collision of this kind at moderate free-fall velocity. The effects of impingement velocity, of the properties of the liquids used, and of the proximity of the container walls are then discussed.

a. Major stages

The major stages in the collision of a 0.2-g waterdrop that fell from a height of 40 cm into a target liquid consisting of milk mixed with water are given below [6, 7]. For convenience of later reference, successive stages in the collision are arbitrarily identified by capital letters.

(A) As the drop collides with the target liquid, a little cup of liquid, having small protruding spicules of liquid around its mouth, is thrown up around the trailing end of the drop, which is not appreciably distorted. This cup of liquid grows wider and higher to form a short bellmouthed[b] cylinder of liquid above the target liquid at the periphery of a (more or less hemispherical) cavity that forms in the target liquid.

The drop that impinged apparently rides down into the target liquid on the receding surface of the floor of this cavity as the cavity grows in size. As the drop rides down into the target liquid it also flows out radially so that the interior both of the hemispherical cavity,

---

[b] The term "bellmouthed cylinder" is used to designate a cylindrical shape with a flared end.

which forms in the target liquid, and the interior of the bellmouthed cylinder of liquid, which stands at the periphery of this hemispherical cavity, are lined with liquid that originally belonged to the drop.

The bellmouthed cylinder of liquid at the periphery of the cavity rises rapidly and its walls thicken. The spicules of liquid, which originally sloped outward at the mouth of this cylinder of liquid, neck off small drops and contract to form lobes of liquid.

(B) After the cavity in the target liquid has grown to maximum size, it begins to collapse. During the collapse process, it increases in size radially while it simultaneously shallows; the cylinder of liquid at its periphery recedes toward the surface of the target liquid. After a total elapsed time of about 55 msec, all that remains on the surface of the target liquid is a ring of lobes surrounding a central hollow.

(C) When the total elapsed time is about 65 msec, a jet of liquid begins to rise from the center of the residual hollow in the target liquid. A picture of the jet just emerging from the target liquid is shown in figure 1. This jet carries at its summit the liquid of the drop that impinged. It reaches a maximum height after approximately 116 msec, and, due to instability, shows a tendency to neck off a drop.

(D) After reaching maximum height this jet subsides. As it recedes toward the surface of the target liquid, a mound of liquid collects at its base. The edge of this mound of liquid spreads outward in an ever-widening circular ripple. By the end of 217 msec the head of this first jet sinks into the mound of liquid that collected at its base. The final subsidence of the jet gives rise to a vortex ring that descends through the liquid.

(E) If the first jet does not neck off a drop, its disappearance is quickly followed by the rise of a second jet of different shape after a total elapsed time of about 240 msec. This jet also subsides forming a mound of liquid on top of the mound that was formed during the subsidence of the first jet, and this mound of liquid forms a ripple that follows after the first one.

If, however, the summit of the first jet necks off a drop (or even nearly necks off a drop) the impact of this drop forms a crater in the top of the mound of liquid that formed during the subsidence of the first jet, and the rim of this crater spreads outward to form a second ripple, which, in this case, quickly follows the first one. The second jet then forms in the center of this crater, but it forms at a later time than it did for the case that a drop did not neck off the first jet.

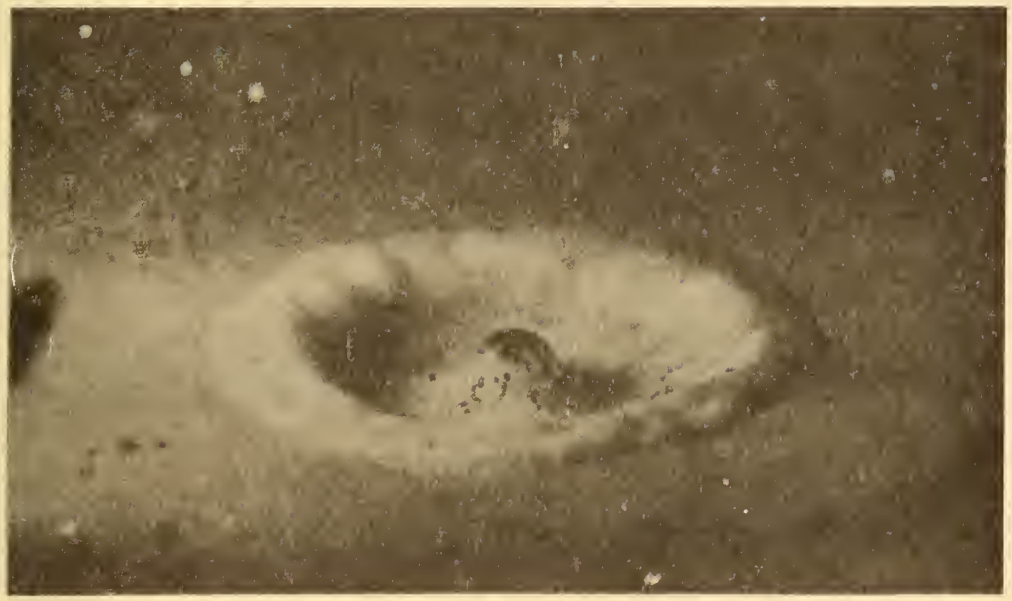

FIGURE I. CENTRAL JET EMERGING FROM FLOOR OF SUBSIDING CAVITY IN TARGET LIQUID

b. Effect of velocity

In stage (A), for collisions at very low velocity, the drop that impinged only moves out radially to the extent of flattening as it rides down into the target liquid on the receding surface of the floor of the cavity that is produced by the collision [5]. It eventually sinks into the target liquid at the bottom of the cavity but later reappears in a flattened lobed form and becomes the summit or head of the jet of liquid that rises [5].

In stage (A), for collisions at relatively high velocity, the drop flows out radially as it rides down into the target liquid on the receding surface of the cavity floor [7]. The liquid of the drop is spread out in a thin lining over the interior of the hemispherical cavity and over the inside walls of the bellmouthed cylinder of liquid that rises at the periphery of the cavity [7]. See section 1.2.a.

For collisions at even higher velocity the cylinder of liquid that exists at the periphery of the cavity in stage (A) rises to a considerable height and its top constricts, as though it were pulled in by a drawstring, to form a dome of liquid over the cavity [6, 7]. Whether or not this surface closure occurs seems to depend on the mass as well as on the velocity (height of fall) of the drop [7]. Closure of the liquid cylinder is sometimes either incomplete or only temporary, and the liquid dome reopens at the top to make way for the rising jet of liquid in stage (C); the liquid jet is thick and of low height [7]. If the liquid dome does not reopen the rising jet strikes the dome and bursts through it [7].

Worthington [6, 7] explained the constriction of the top of the liquid cylinder to form a liquid dome as being the result of surface tension. He suggested, however, that surface tension may not be the only cause and that the cylinder may be in part forced in by excess external air pressure because of the lessening of air pressure within it that is produced by the deepening of the cavity in the target liquid [6].

In the higher-velocity collisions, which result in the formation of a dome of liquid over the cavity in the target liquid, a downward-moving jet is produced. It seems to have its origin at the apex of the liquid dome, where closure occurs, and its movement is toward the cavity floor. Worthington [7] observed this downward jet in the case of collisions of solid spheres with liquids but failed to observe it in his study of the collision of liquid drops with liquids. The existence of this jet is clearly visible in pictures taken by Franz [9] who was interested in the sounds produced by these collisions and did not make an analysis of the collision events themselves.

c. Effect of properties of the liquids used

If the properties of the liquid used for projectile and target are notably different, the stages in the collision are similar but the extent to which they progress is changed.

With regard to the effect of a change in surface tension of the target liquid, Worthington [6] stated that addition of milk to the water into which a waterdrop fell did not make a noticeable change in the phenomena if the addition was only to the extent of producing a 1 to 3 ratio of milk to water; if pure milk was used, the liquid cylinder thrown up (see stage A) was higher and had longer spicules indicating a smaller efficiency of the surface tension in opposing the rise of the liquid.

With regard to a change in the viscosity of the target liquid, Worthington [5] stated that the stages in the collision when a drop of milk falls into petroleum or olive oil are similar to those that result when it falls into water, modified, however, by the greater or less mobility of the liquids in question.

d. Effect of proximity of container walls

The effect on the stages of the collision of the proximity of the walls of the vessel that contained the target liquid has not been discussed. The observations of Franz [9] were obtained using a 91.4-cm (3-ft)-square glass-walled tank 152.4 cm (5 ft) high that was nearly filled with water. The target-liquid reservoir used by Edgerton and Killian [8], who were primarily interested in the qualitative aspects of the collision from the standpoint of high-speed photography, appears, from their pictures, to have been about the size of a drinking glass. The glass vessel with parallel sides that was used by Worthington [7] to photograph the stages of the collision below the surface was an inverted clock shade.

May [10] has investigated the effect of proximity of container walls on the water-entry behavior of solid spheres. He has concluded that, within the range of his investigation, it appears that wall effects will be avoided if the width of the target-liquid tank is at least five times the maximum width of the cavity that is formed on entry.

The effect of this variable in collisions of liquid drops with liquids should be of considerable interest with regard to cavities formed by meteor collisions. If liquefaction occurs as a result of meteor collisions, as has been postulated [1], it will probably be restricted to the immediate site of the collision.

2. CORRELATION WITH HYPERVELOCITY-PELLET AND METEORITE CRATERS

In this section several aspects of cavities produced in collisions of liquid drops with liquids, which have been reported in the preceding section, are correlated with aspects of craters produced in hypervelocity and meteor collisions, to which they may bear some relation.

Worthington [7] observed that, in high-velocity collisions of liquid drops with liquids, the cavity formed in the target liquid was hemispherical and that the liquid belonging to the drop that impinged flowed out radially and lined both the hemispherical cavity and the bellmouthed cylinder of liquid that formed at the periphery of this cavity. Similarly, it has been observed that craters produced by hypervelocity collisions of metal pellets with metal targets are, in general, approximately hemispherical [2]. Evidence that the material of the pellet may flow out radially to form a lining in the hemispherical cavity [11] or be plated on the inside of the crater [2] also exists.

The bellmouthed cylinder of liquid that rises at the periphery of the cavity in the target liquid provides another basis for comparison. This bellmouthed cylinder is shown in panels a, b[a], and c[b] of figure 2 for three types of collision, namely, for a 182-mg waterdrop colliding with water at 700 cm/sec, for a 2.54-cm (1-in.) steel sphere colliding with water at 1,100 cm/sec, and for a 0.3175-cm (1/8-in.) 302 stainless steel sphere colliding with a 2024-T4 aluminum target plate at hypervelocity, respectively. In panels a and b the cavity below the surface can be seen through the transparent target liquid; in panel c only the bellmouthed cylinder of metal above the surface of the opaque aluminum target plate can be seen. There is a strong similarity in the appearance of the structure above the surface of the target for the three types of collision; differences correlate with the velocity at which the collisions occurred.

Because the steel sphere shown in panel b of figure 2 did not flow out as a result of the collision, the bellmouthed cylinder of liquid seen in panel b is composed entirely of the target liquid which was water. In panel a, on the other hand, the bellmouthed cylinder of liquid that was thrown up by a waterdrop colliding with water is lined with water that belonged to the drop because the drop flows out radially during the collision. In panel c, the bellmouthed cylinder of metal thrown up in the hypervelocity collision may or may not be lined with metal that belonged to the colliding sphere depending on the extent to which liquefaction of the 302 stainless steel sphere and the 2024-T4 aluminum target has progressed.

---

[a] These pictures were supplied by Dr. Albert May, U. S. Naval Ordnance Laboratory, White Oak, Maryland.

[b] These pictures were supplied by Lt. Thomas E. Sheldon, Headquarters Air Proving Ground Center, Eglin Air Force Base, Florida.

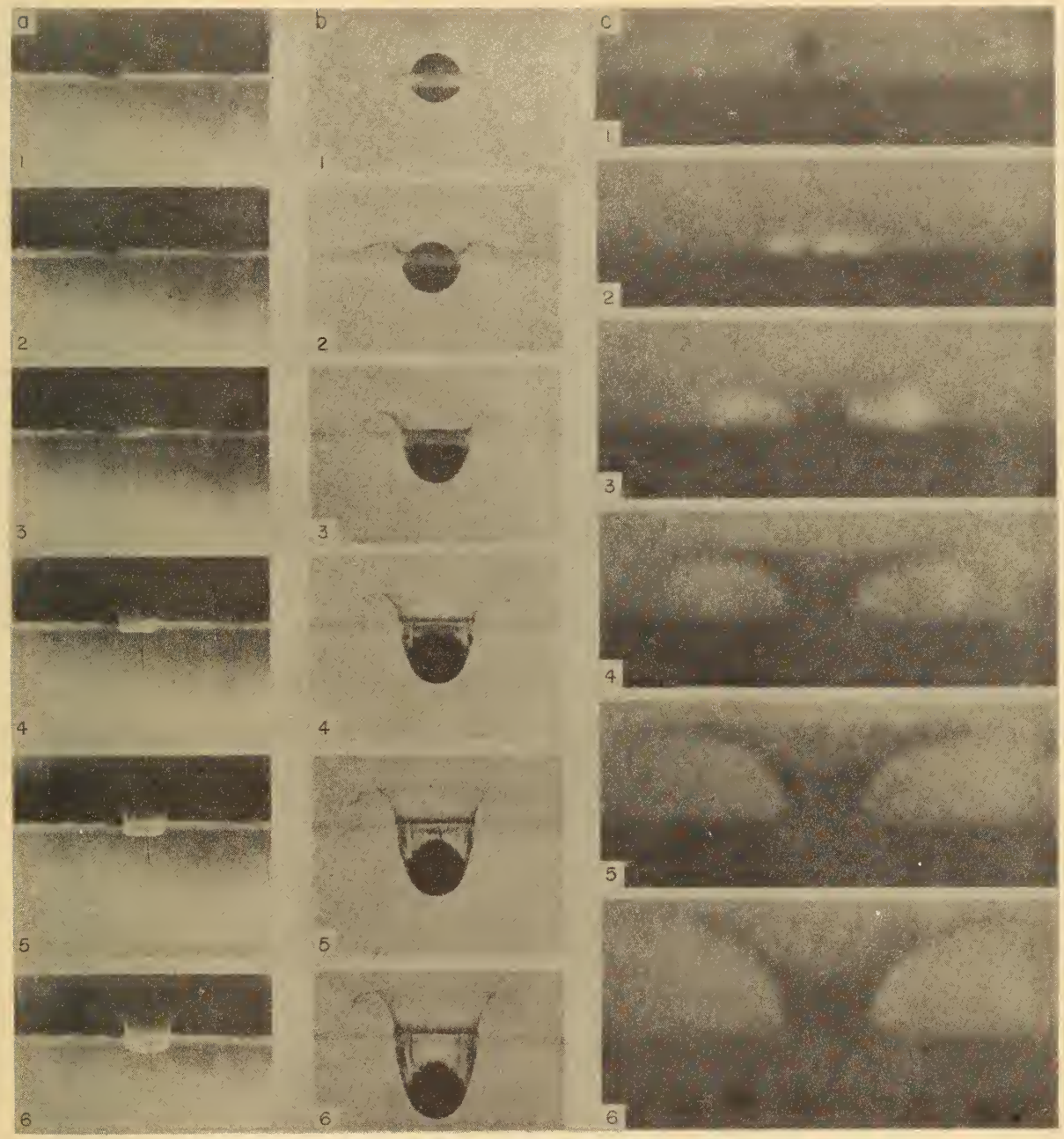

FIGURE 2. INITIAL STAGES OF THREE TYPES OF COLLISION

To account for the curling-over of the liquid thrown up around the cavity, Worthington [6] stated that at first the flow of liquid appears to be very much along the surface whereas at a later time it is much more perpendicular to the surface, and that in the early stages each particle continues to move for some distance in the straight line along which it was first projected from the surface.

In figure 2, the extent of curling-over of the cylinder of liquid around the cavity is greatest for the highest-velocity collision (panel c) and is least for the lowest-velocity collision (panel a); the height of the bellmouthed cylinder of liquid with respect to the diameter of its base is in the same order.

It has been suggested that the craters on the moon may have been caused by impinging meteors. Lunar craters 1) are cuplike depressions with steep inside slopes that decrease gradually to a nearly level floor depressed below ground level; 2) the volume of the rim is equal to the volume of the subsurface part of the crater; 3) some of the craters contain a central peak whereas others do not; and 4) some craters have a system of rays about them [12]. Official U. S. Navy photographs of some craters on the moon are shown in figure 3[c]. Baldwin [12] has concluded that lunar craters are explosion pits. However, the four attributes of lunar craters cited above may correlate with stages in collisions of liquid drops with target liquids.

With regard to the first two attributes, at the time that the first liquid jet begins to emerge (see section 1.2.a and fig. 1), the hemispherical cavity that originally formed in the target liquid has become wide and shallow. Compression in the target liquid has been relieved and it is reasonable to suppose that the volume of the residual crater is roughly equivalent to the volume of the rim that surrounds it.

With regard to the third attribute, if meteor collisions are a kind of liquid-drop liquid-target collision, and if the liquid melt caused by the high-speed collision should freeze just as the jet began to protrude from the bottom of the cavity (see fig. 1), the frozen structure would be a crater containing a central protuberance; if the liquid melt froze just before the head of the jet emerged from the bottom of the cavity, the frozen structure would be a crater without a central protuberance. The liquid crater shown in figure 1 may be compared with lunar craters that contain a central protuberance. Such craters are marked with arrows in figure 3.

---

[c] These photographs were supplied by Mr. J. L. Gossner of the U. S. Naval Observatory in Washington, D. C.

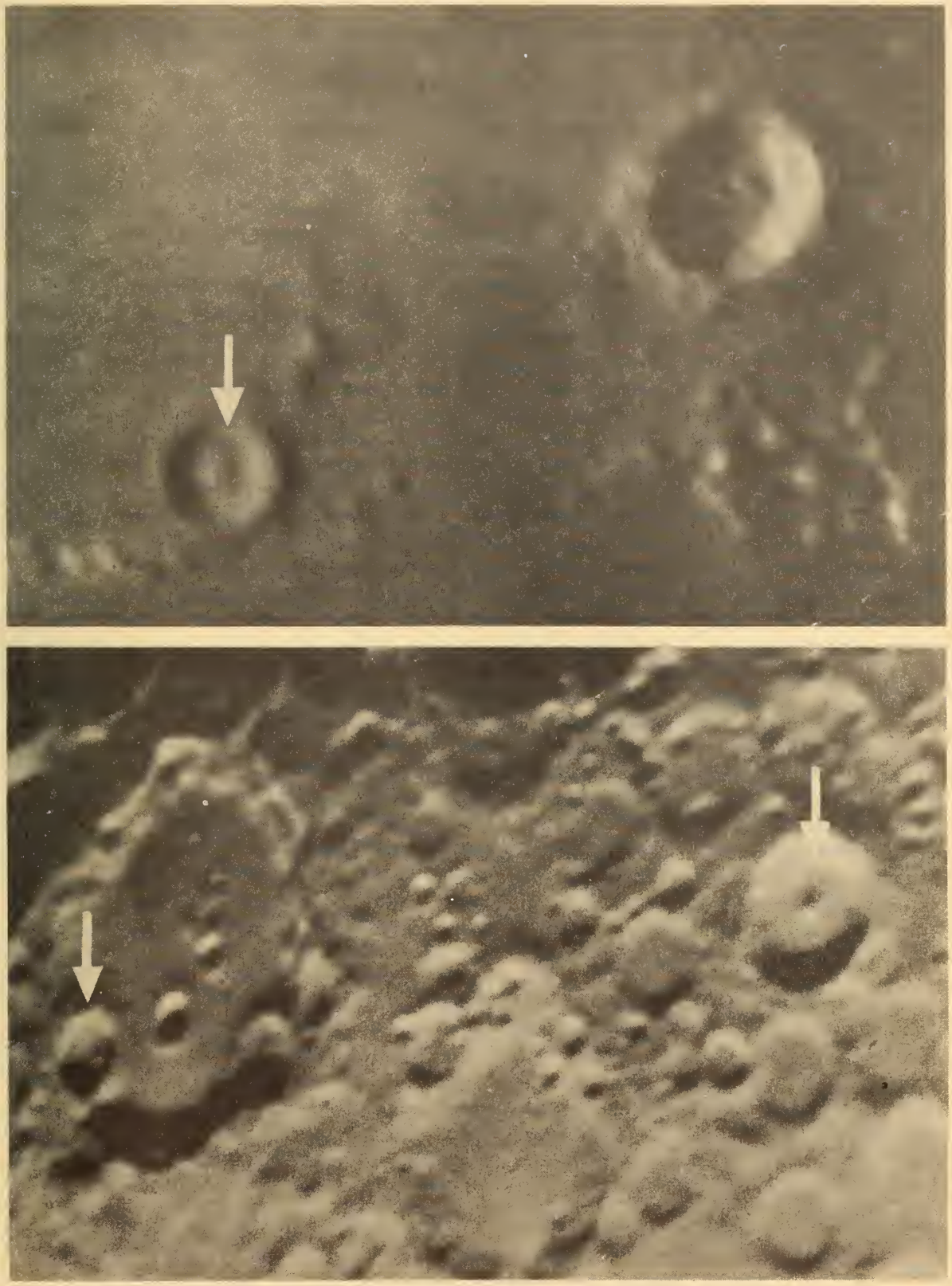

FIGURE 3. CRATERS ON THE MOON

With regard to the fourth attribute, Worthington [5] remarked that symmetrical rays form in the cavity that develops in the target liquid when a liquid drop collides with a liquid. As seen in his sketches, these rays terminate in projecting points around the rim of the cavity.

3. QUANTITATIVE DATA ON LIQUID-DROP-INTO-LIQUID COLLISIONS

Worthington [6] made a first step toward obtaining quantitative data. He followed the time required for accomplishment of the various stages of the collision of a 0.2-g waterdrop that fell 40 cm into a target liquid of milk mixed with water. He found that the cylinder of liquid at the periphery of the cavity rose to its maximum height in 20 msec and remained poised with little change for the next 10 msec. It then widened out and subsided until nothing but a lobed rim surrounding a central hollow was left above the surface; this required 25 msec. The subsidence of the liquid cylinder was followed by the rise of the central jet, which required 50 msec, and by its subsidence, which required 70 msec. The total time accounted for was 175 msec. These stages of the collision, therefore, took place in less than one fifth of a second.

For a theoretical analysis of this type of collision, more quantitative data are needed. The very limited quantitative study of the collision incident that is presented in this section has been made with the use of the high-speed motion pictures of waterdrops falling into water that were taken by Franz [9] in connection with his study of the sounds that are produced. His kind loan of these motion picture films, for whatever other data could be derived from them, is gratefully acknowledged.

The films that were made available comprised collisions of three sizes of drops for two combinations of drop mass with collision velocity: 11-mg drop colliding at velocities of 400 and 650 cm/sec, 56-mg drop colliding at velocities of 400 and 700 cm/sec, and 182-mg drop colliding at velocities of 400 and 700 cm/sec. The stages in the collisions are similar to those described in section 1.2.a. Pictures of the stages of similar collisions have been given by Franz [9]. The collisions of the 56-mg and 182-mg drops at a velocity of 700 cm/sec resulted in surface closure of the cavity in the target liquid in a way similar to that described in section 1.2.b.

For the purpose for which the films used in this study were made, there was no need to photograph a reference standard of length or of optical distortion in the system. That this was not done, however, reduced the accuracy with which the cavity depth and diameter measurements reported below could be determined. Nevertheless, the data obtained from these films are valuable in giving the broad outlines of some quantitative aspects of this type of collision, and in indicating points that should be studied in future experiments.

3.1 Cavity Depth

Measurements of the depth of the cavity in the target liquid, at known intervals of time after the collision incident, were made on magnified prints of the motion picture films. These prints were obtained with use of a microfilm reader-printer. The measurements were made using a stereomicroscope set for low magnification and a steel rule graduated to 1/2 mm. Each recorded measurement is the average of two readings.

The meniscus appeared as an indistinct line in the prints. The mid-point of this indistinct line was arbitrarily taken to be the undisturbed surface of the target liquid. The depth of the cavity was measured with respect to it. The fact that the bottom of the cavity and the periphery of the mouth of the cavity at the surface of the liquid were also indistinct reduced the accuracy with which the measurements could be made.

The time that had elapsed from the first instant of the collision was found from the reported speed at which the pictures were made. This was 2,800 frames/sec or 357 μsec per frame.

To convert measured values of cavity depth to real values, the magnifying factor was determined for the prints made from each film. For the case that the freely falling drop was spherical, the magnifying factor was taken to be the ratio of the real diameter of the drop to the measured diameter. The real diameter was calculated from the volume of a sphere and the reported mass of the drop, taking the density of the water used to be one. For the case that the freely falling drop was an oblate spheroid, the magnifying factor was taken to be the ratio of the real major axis of the drop, calculated from its mass, to the measured major axis. The real major axis was calculated from the volume of an oblate spheroid, the ratio of the measured semi-major to the measured semi-minor axis of the drop, and the reported mass of the drop, taking the density of the water used to be one.

The cavity-depth data are plotted in figure 4. Curves A and A' are for the 11-mg drop colliding at velocities of 400 and 650 cm/sec, respectively; curves B and B' are for the 56-mg drop colliding at velocities of 400 and 700 cm/sec, respectively; curves C and C' are for the 182-mg drop colliding at velocities of 400 and 700 cm/sec, respectively.

From figure 4 it can be seen that for each of the collisions the cavity that forms in the target liquid undergoes a relatively smooth increase in depth until maximum depth is approached. At the time of maximum depth, the cavity appears to vibrate. Each curve of figure 4 has been drawn arbitrarily through the vibration fine structure so that the maximum of the curve is the average depth of the cavity at the time of maximum depth. The maximum of the curve of cavity depth versus time is hereafter referred to as the maximum depth of cavity produced.

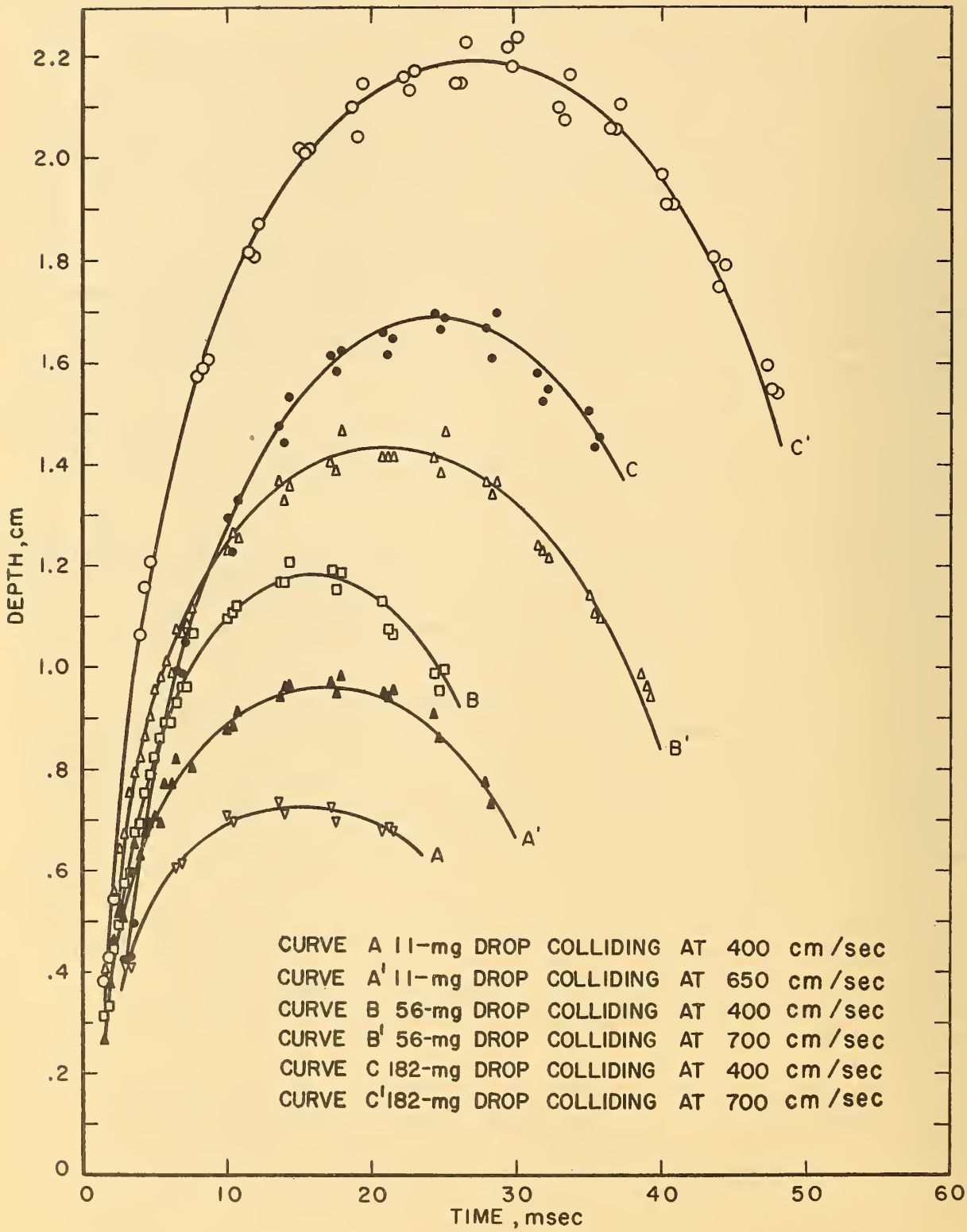

FIGURE 4. DEPTH OF CAVITY PRODUCED IN WATER BY AN IMPINGING WATERDROP PLOTTED AGAINST ELAPSED TIME

By comparing curve A with A', curve B with B', and curve C with C' it can be seen that increasing the collision velocity with drop mass constant in each case increases both the maximum depth of the cavity produced in the target liquid and the time that was required to produce maximum depth. Similarly, by comparing curves A, B, and C, or curves A', B', and C', it can be seen that increasing the mass of the drop with collision velocity constant also results in an increase both in the maximum depth of the cavity produced in the target liquid and in the time required for the cavity to grow to its maximum depth. By comparing curve B with curve B', and then comparing curve B' with curve C', it appears that an increase in the mass of the drop may be less important than a proportional increase in collision velocity in producing the effect of increase in maximum cavity depth and of increase in the time required to produce maximum depth.

The maximum depth of cavity produced and the time required to reach this maximum cavity depth for each of the six collisions that have been studied are listed in table 1 and plotted in figure 5.

The plots of cavity depth versus time shown in figure 4 appear to be parts of a family of parabolas or ellipses tangent to the cavity-depth axis at the origin[f]. The general equation of a family of ellipses is

$$\frac{D^2}{a^2} + \frac{(t - b)^2}{b^2} = 1 \qquad (1)$$

where D is the cavity depth, t is the time, a is the semi-major axis, and b is the semi-minor axis. When the cavity depth D is zero, $t = 0$ and $t = 2b$. The semi-major axis is the maximum cavity depth produced, D_m, and the semi-minor axis is the time required to produce the maximum cavity depth, t_m. Solving eq (1) for cavity depth D produces the expression,

$$D = a \left(2 - \frac{t}{b}\right) (t/b)^{1/2}. \qquad (2)$$

The cavity-depth-versus-time data for the 56-mg waterdrop colliding with water at a velocity of 700 cm/sec is plotted in figure 6 with the curve calculated by use of eq (2). In calculating points by eq (2), the

---

[f] A theoretical analysis of this aspect of collisions of liquid drops with liquids is in progress.

Table 1

Properties of the Cavity at Maximum Size

Projectile Drop		Cavity Depth, D	Elapsed Time, t	Cavity Depth divided by Cavity Diameter
Mass mg	Velocity cm/sec	mm	sec	
11	400	7.25	0.0139	0.64
11	650	9.70	0.0168	0.58
56	400	11.9	0.0161	0.56
56*	700*	14.4*	0.0207*	0.55*
182	400	16.8	0.0246	0.52
182*	700*	21.9*	0.0286*	0.54*

* Surface closure of the cavity occurred.

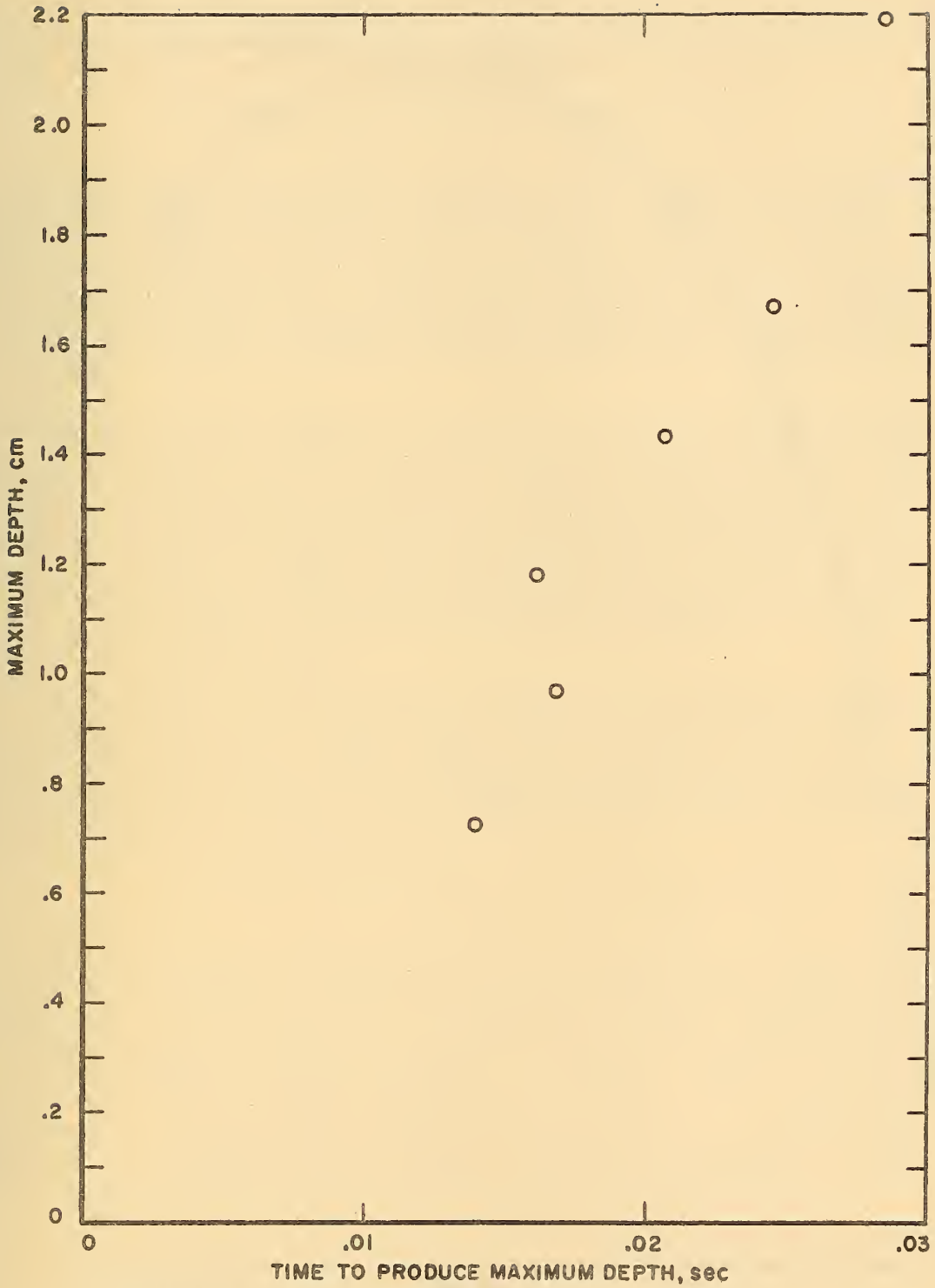

FIGURE 5. MAXIMUM DEPTH OF CAVITY PRODUCED IN WATER BY IMPINGING WATERDROPS PLOTTED AGAINST THE TIME REQUIRED TO REACH IT

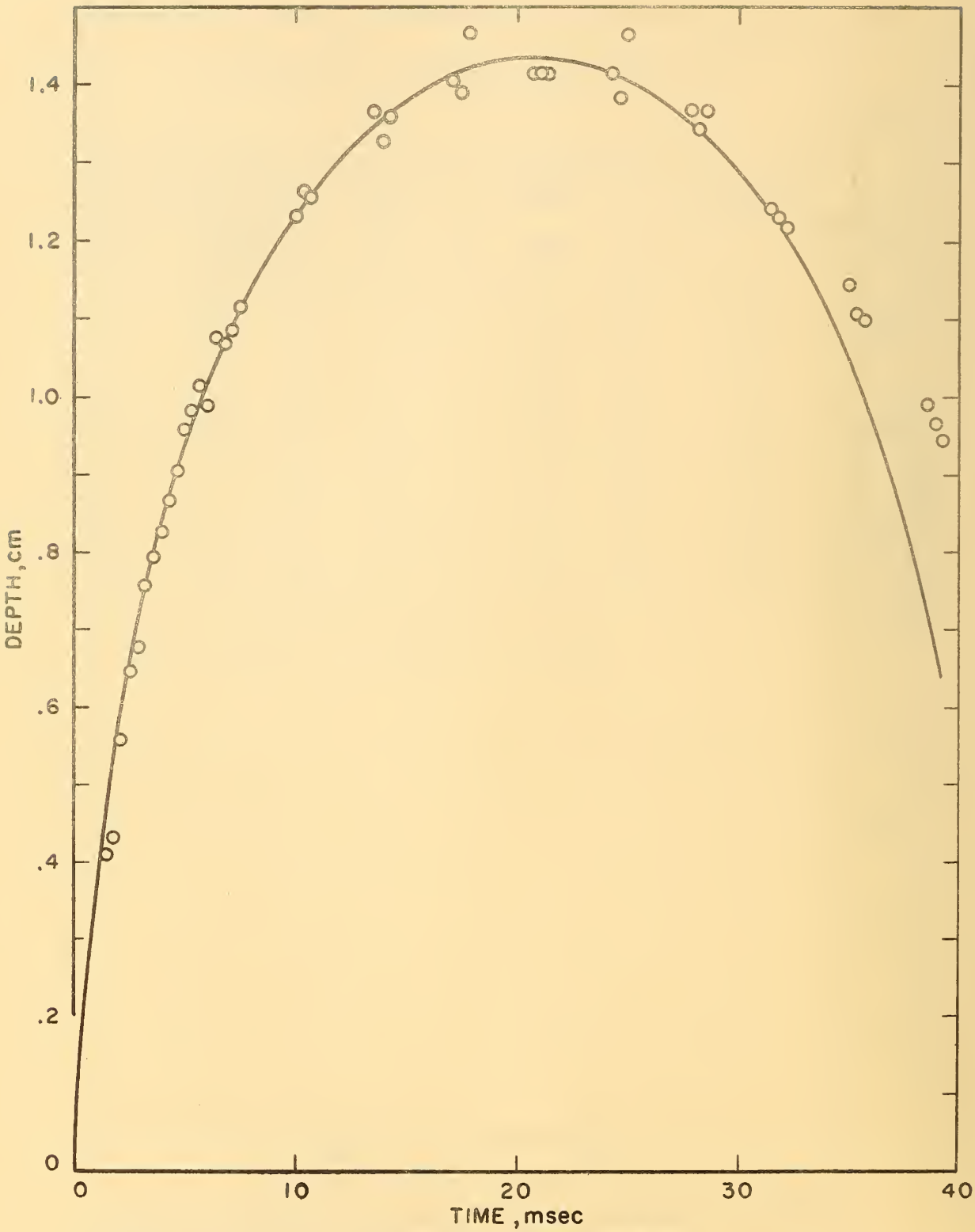

FIGURE 6. DEPTH OF CAVITY PRODUCED IN WATER BY COLLISION OF 56-mg WATERDROP AT 700 cm/sec PLOTTED AGAINST ELAPSED TIME

empirical values of D_m and t_m for this collision were used. The divergence of the observed values from the calculated curve after 32 msec may be the result of energy dissipation (hysteresis).

3.2 Ratio of Cavity Depth to Cavity Diameter

Measurements of the diameter of the cavity produced in the target liquid were made at intervals of time after the collision for which depth measurements had been made. The diameter that was measured was the maximum diameter at the surface of the target liquid. Both the cavity depth and the ratio of cavity depth divided by cavity diameter are plotted in figure 7 against the time elapsed since the collision for the collision of the 182-mg waterdrop with water at a velocity of 400 cm/sec.

From the plots of figure 7 it can be seen that the depth/diameter ratio for the collision of a liquid drop with a target liquid is not constant with time. It goes through a maximum and it reaches its maximum sooner than the depth curve does. From the depth/diameter curve plotted in figure 7 it would appear that this ratio is equal to 0.5 only at two points in time. For very short times after the collision, the cavity is oblate; just before and also during the time that it reaches maximum depth, it is prolate; during the stages of its subsidence, it is again oblate.

Depth/diameter curves for the other five collisions for which data were available were of a similar shape. The maximum value of the curves ranged from 0.55 to 0.65. Small differences in these curves may or may not be significant; more data are needed to evaluate them. The value of depth/diameter at the time of maximum cavity depth is listed in table 1 for each of the six collisions.

3.3 Effect of the Energy of the Impinging Drop

The total energy of each drop that collided with the target liquid is the sum of its kinetic energy and surface energy. The kinetic energy of each drop was calculated from the mass and velocity reported for it. The surface energy of each drop was found from the calculated surface of the drop taking the surface tension of the water used to be 72.75 dyne/cm. For the case that the freely falling drop appeared to be a sphere, the surface area of the drop was taken to be πd^2 where d is the drop diameter; for the case that the freely falling drop appeared to be an oblate spheroid, the surface area of the drop was taken to be $2\pi a^2 + \pi b^2/e \, [\ln (1 + e)/(1 - e)]$ where a is the semi-major axis, b is the semi-minor axis, and the eccentricity e is $(a^2 - b^2)^{1/2}/a$. The values of d, a, and b were calculated. See section 3.1.

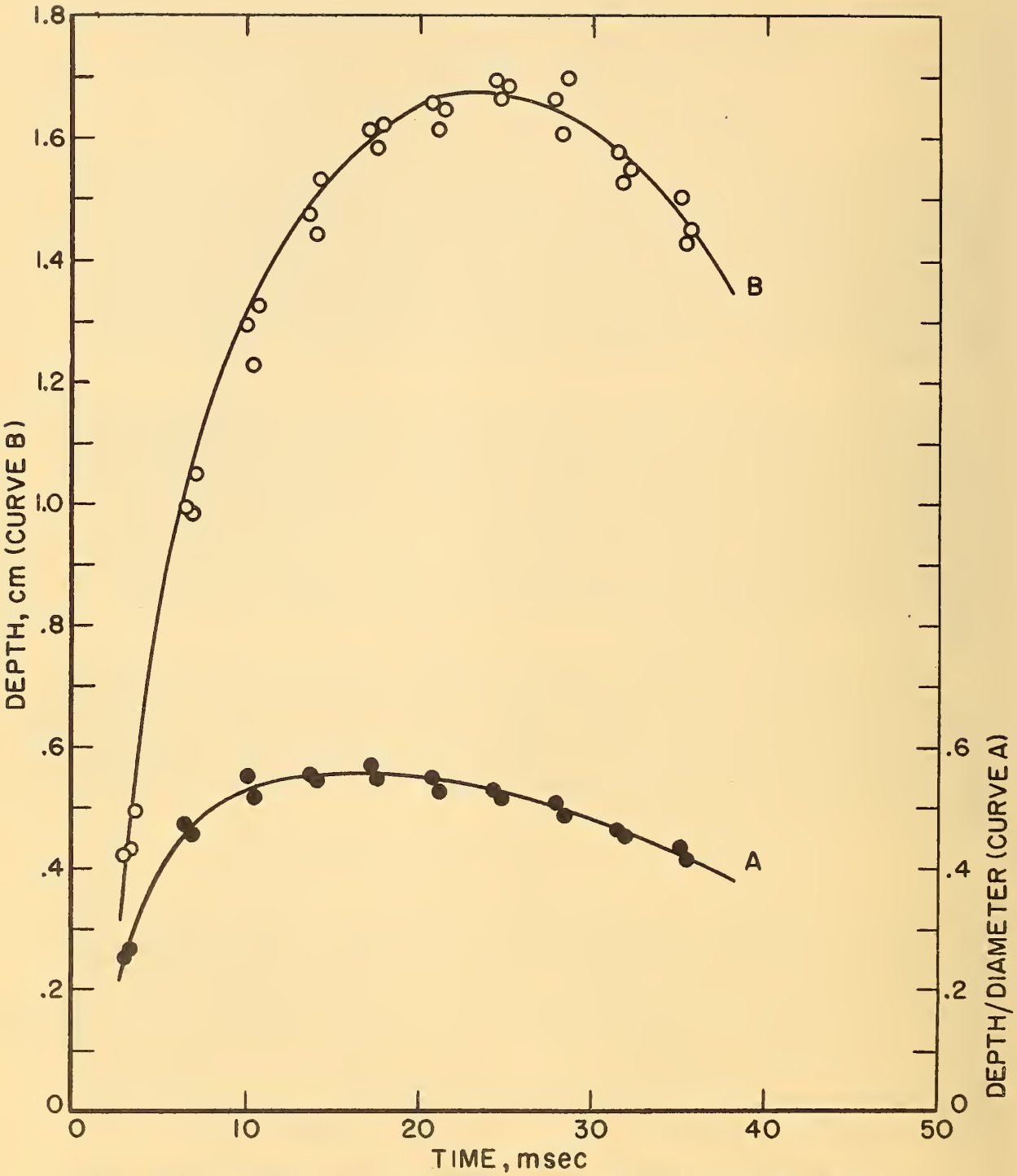

FIGURE 7. DEPTH AND DEPTH/DIAMETER RATIO OF THE CAVITY PRODUCED IN WATER BY COLLISION OF A 182-mg WATERDROP AT 400 cm/sec

The kinetic energy, surface energy, and momentum of the impinging drop for each of the six collisions for which data were available are given in table 2. The total energy is not tabulated. The values of the kinetic energy and of the surface energy are both good to two significant figures, but the magnitude of the values is so different that the surface energy becomes insignificant if it is added to the kinetic energy.

The observed value of maximum depth of the cavity produced in the target liquid is plotted against the kinetic energy of the colliding drop in figure 8 and against the momentum of the drop in figure 9. Points for the two collisions for which surface closure of the cavity occurred are marked with a cross in each graph because maximum cavity depth may be affected when surface closure occurs. For these collisions the mouth of the cylinder of water thrown up around the cavity in the target liquid constricted and eventually closed to form a dome of liquid over the cavity. See section 1.2.b.

From a practical standpoint it would be informative if the relation between the energy of the impinging drop and the maximum depth of the cavity produced in the target liquid as a result of the collision could be ascertained. It has been found [2] that, in the fluid region of hypervelocity collisions of metal pellets against metal targets, the volume of the crater formed in the target is proportional to the kinetic energy of the impinging pellet; the craters formed are also nearly hemispherical in shape. If it is assumed that, at the time of maximum depth, the volume of the cavity in the target liquid is proportional to the kinetic energy of the impinging drop, then, for a spherical drop that produces a hemispherical cavity,

$$D_m = K r (\rho V^2)^{1/3} \qquad (3)$$

where D_m is the maximum depth of the cavity, r is the radius of the original drop, ρ is the density of the drop liquid, V is the impingement velocity, and K is a constant having the dimensions $(\text{cm}\cdot\text{sec}^2/\text{g})^{1/3}$ which are those of the cube root of reciprocal pressure. For the case that $\rho = 1$,

$$D_m = K r V^{2/3} \qquad (4)$$

For a drop whose shape is an oblate spheroid,

$$D_m = K (a^2 b)^{1/3} V^{2/3} \qquad (5)$$

where a and b are the semi-major and semi-minor axes, respectively.

Table 2

Energy and Momentum of the Impinging Waterdrops

Drop Mass g	Drop Velocity cm/sec	Momentum g.cm/sec	Kinetic Energy ergs	Surface Energy ergs
0.011	400	4.4	880	17.4
0.011	650	7.2	2,300	17.4
0.056	400	22.	4,500	51.5
0.056	700	39.	14,000	51.8
0.182	400	72.8	14,600	115.
0.182	700	127.	44,600	113.

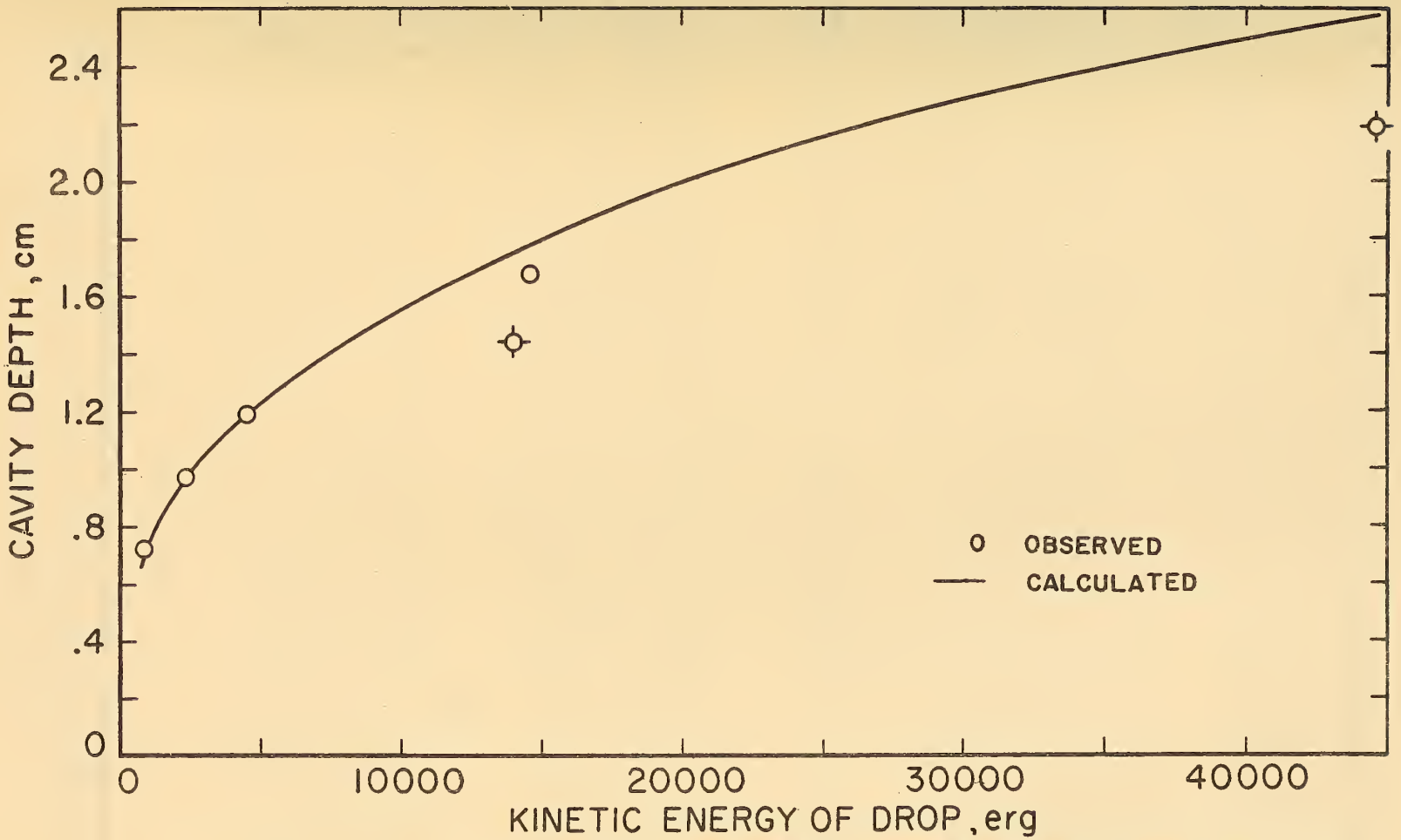

FIGURE 8. DEPTH OF CAVITY PRODUCED IN WATER BY IMPINGING WATERDROPS PLOTTED AGAINST THE KINETIC ENERGY OF THE DROPS

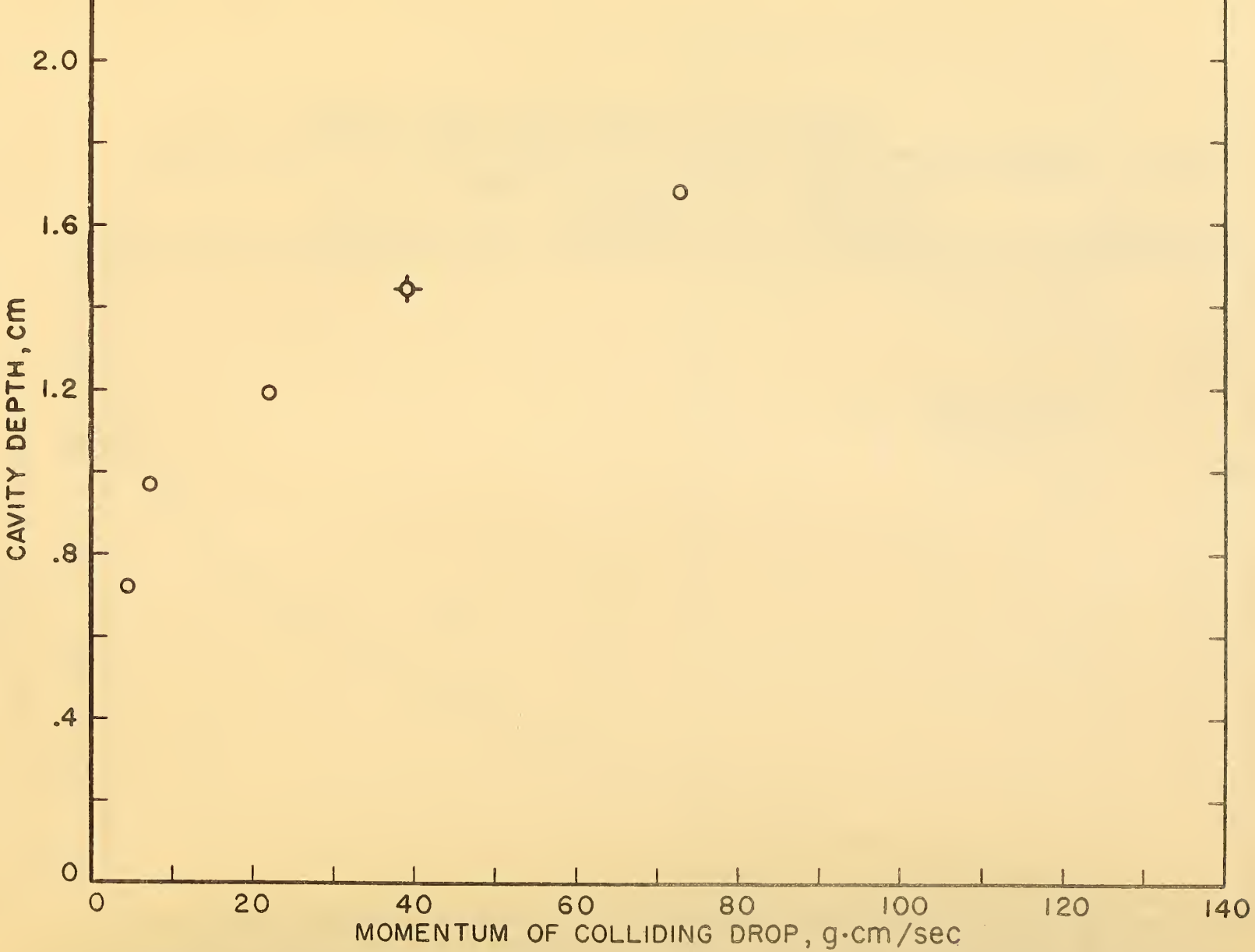

FIGURE 9. DEPTH OF CAVITY PRODUCED IN WATER BY IMPINGING WATERDROPS PLOTTED AGAINST THE MOMENTUM OF THE DROPS

The equation can be tested with the available data by determining whether or not K remains constant. In the experiment in which the moving pictures were obtained [9] the waterdrops were allowed to fall through air. The three drops having lowest kinetic energy were spherical in shape at the time that they collided with the target liquid; the three drops having highest kinetic energy were oblate spheroids. The values of the constant K, calculated with use of eqs (4) and (5) and the empirical values of D_m are listed in table 3.

The data for the two collisions that resulted in surface closure of the cavity in the target liquid are marked with asterisks in table 3. Because maximum cavity depth may be affected for the case that surface closure occurs, the values of K that are marked with asterisks in table 3 may be disregarded in evaluating the constancy of K. However, even if the two values of K that are marked with asterisks are ignored, the tabulated values suggest that K may not be constant. It appears to be decreasing as the kinetic energy of the drop is increased but more data are needed to determine whether or not the drift is real.

The average value of K for the four collisions for which surface closure did not occur is 0.093. Points calculated by use of eqs (4) and (5) and with K = 0.093 are connected with a line in figure 8.

4. CURRENT RESEARCH

Although 80 years have passed since Worthington [5] started his investigation of collisions of liquid drops with liquids, it can be seen from the preceding sections that even the simplest example of this type of collision (waterdrops falling into water) is very poorly understood. High-speed photography is the tool needed to obtain further information. More high-speed motion pictures, taken under conditions and with controls that will make it possible to evaluate the accuracy of measurements made on them, are required.

Apparatus with which an exhaustive study of collisions of liquid drops with liquids can be made is now being assembled at the National Bureau of Standards. It consists essentially of a 15.2-cm (6-in.)-diam pipe that is 20 m (66 ft) long attached to a sealed tank that contains the target liquid. The purpose of the pipe is to provide gravity acceleration of the liquid drops under reduced pressure. The system is being assembled in a stairwell. The target-liquid tank is located at the basement level; the pipe extends through four stories of the building and terminates in the penthouse.

4.1 Evacuated System

To increase the kinetic energy of the projectile drop either its velocity, or mass, or both must be increased. The velocity acquired by a drop for any given height of fall will be greater in an evacuated

Table 3

Values of the Proportionality Constant K

Drop Mass g	Drop Velocity cm/sec	Constant K $(cm.sec^2/g)^{1/3}$
0.011	400	0.097
0.011	650	0.094
0.056	400	0.092
0.056*	700*	0.077*
0.182	400	0.088
0.182*	700*	0.079*

* Surface closure of the cavity occurred.

system than in air because of the reduction in drag. The size of the drop can also be made larger in an evacuated system than in air because the tendency for breakup due to air currents encountered during fall will be reduced. The lowest feasible pressure for the simple system in which both the drop and target are of the same liquid is the room-temperature vapor pressure of the liquid selected for study. If the pressure in the system were to be made lower than this, both the target liquid and the projectile drop would boil.

The drop-accelerator pipe and the target-liquid tank have been designed so that both the volume of the pipe and the free space above the target liquid in the tank can be exhausted to the vapor pressure of the liquid under study. The evacuation will be accomplished by means of an air-cooled simplex-type vacuum pump having a free air displacement of 36.8 l/min (13 cu ft/min). Because the vapor pressures of the liquids to be used will be in the millimeter range, pressure in the system will be checked by means of a mercury manometer.

The end of the pipe is connected to the target-liquid tank through a 15.2-cm (6-in.) aluminum ball valve. With the ball valve closed, the pipe can be evacuated without concomitant evaporation of the target liquid and the consequent need to trap out large quantities of vapor. Vapor must be trapped out when the free space above the target liquid is evacuated, but the volume involved is not large. After the pipe and tank have been evacuated separately, the valve between them will be opened and the target liquid will be allowed to evaporate until equilibrium is reached.

The throat of the connecting ball valve is large enough so that drops, falling through the pipe, can pass through it and strike the target liquid in the tank below. The valve is equipped with natural rubber seats and seals to insure long service life in the atmosphere saturated with water vapor that will exist within the system.

4.2 Materials

The drop-accelerator pipe and target-liquid tank are both made of 5052 aluminum alloy to minimize corrosion and changes in the properties of the liquid under study that corrosion might produce. This aluminum alloy has been used for distilled water lines. Welding for the system was done with 5154 aluminum rod. Small model tanks made of 5052 aluminum sheet and welded with either 5154 or 5356 aluminum rod were each found to be vacuum tight on the first trial when tested with a helium leak detector. Both of these aluminum welding rods were considered satisfactory for corrosion resistance.

The inside surface of the target-liquid tank was coated with black pigmented Epon 820 epoxy resin to reduce light reflection when high-speed shadowgraph motion pictures are taken of the liquid-drop collisions. The tank was then baked at 70°C (158°F) to cure the coating. The epoxy coating will not contaminate the liquids to be investigated.

Vacuum seals at flanged joints in the pipe and tank were made with O-rings of Buna-N synthetic rubber of Durometer 70 hardness. The O-rings were cleaned with ligroine and were used without application of grease.

4.3 Design of the Drop-Accelerator Pipe

The drop-accelerator pipe is of seamless circular tubing; it has a 0.64-cm (0.25-in.) wall thickness, an inside diameter of 15.2 cm (6 in.), and a total length of 20 m (66 ft). It consists of four flanged sections with a port between each section and at the top of the pipe; liquid drops can be introduced into the pipe at the four ports. The lengths of the pipe sections are such that the drop-admittance ports occur at about 1.5 m (5 ft) above the floor at each floor level.

a. Drop-admittance ports

The four drop-admittance ports make it possible to study the collision of a fixed drop mass at four widely different velocities. They are 45.7-cm (18-in.) sections of pipe that have a short side arm welded in. The open end of the side arm is flanged, and, when not in use, each port is closed vacuum tight with a flat circular cover that bears against an O-ring.

At the level of the side arm in the drop-admittance port that is being used, the lower section of the pipe is sealed off with a removable circular plate and ring that are supported by a fixed ring welded into the pipe. Vacuum tightness is insured with O-ring seals. In the center of the removable plate there is a tapered hole into which a 19/38 ground glass joint, which is fitted with an O-ring, may be inserted. The ground glass joint supports a dripper for admitting drops of a given size into the evacuated system.

b. Dripper design

The dripper consists of a pipet nozzle, two liquid reservoirs, and two stopcocks. The inner liquid reservoir, which is sandwiched between the stopcocks, is at first empty and the stopcock that separates this reservoir from the evacuated pipe is left open. The outer liquid reservoir is separated from the inner reservoir by the stopcock furthest from the evacuated system; this reservoir is open to atmospheric pressure and is full of the liquid that is to be used. When the system has come to equilibrium, the inner stopcock is closed and liquid is admitted into the inner reservoir from the outer reservoir at the pressure that prevails within the system. Drops are admitted into the system from the inner reservoir.

The stopcocks have been given a special treatment that permits easy turning without the use of grease which might contaminate the drop liquid. Vacuum tightness of the stopcocks is insured either by spring compression or by liquid seals. By using pipets of different nozzle size the mass of the drop that is admitted can be changed.

4.4 Design of the Target-Liquid Tank

The target-liquid tank is a cylinder 35.6 cm (14 in.) in diameter and 55.9 cm (22 in.) high that was rolled from 1.27-cm (0.50-in.) sheet and welded. Two 30.5-cm (12-in.) side arms, which were also rolled and seamed, are welded into it.

a. Criteria for size

The main criterion used in choosing the diameter of the tank was that it should be large enough to bypass the effect of the container walls on the cavities formed in the target liquid by the liquid-drop collisions. On the basis of available information it appeared that a diameter of 25.4 to 30.5 cm (10 to 12 in.) would be adequate for this purpose. Excessive size was avoided both to reduce problems of procurement or fabrication and to minimize the volume of target liquid that would be required for the experiment. The second consideration will be important when liquids other than water are investigated.

b. Optical windows

The open ends of the side arms in the tank terminate in 1.9-cm (0.75-in.) flanges. They are closed vacuum tight with 2.54-cm (1-in.)-thick covers that contain glass windows through which the liquid-drop collisions will be photographed. The windows are of No. 7913 optical grade Vycor glass of shadowgraph quality. The glass blanks, which were furnished with a commercial polish, were made sufficiently flat, symmetrical, and parallel to insure minimum distortion in the pictures.

4.5 Scope of the Experiment

According to present plans, the apparatus will first be used to carry out an exhaustive study of collisions of waterdrops with water. By use of the four drop-admittance ports in the pipe, it is planned to study the collision of a drop of given mass at four different velocities. By changing the nozzle of the pipet in the dripper, it is planned to study the effect of varying the drop mass. By maximizing both the mass and the velocity of the impinging drop, it is planned to explore further the dependence of cavity depth on the kinetic energy of the drop.

By introducing movable glass barriers into the target liquid, it is planned to study the effect of the proximity of walls. By varying the degree of evacuation of the system, it is planned to study the effect of a change in pressure.

If it is possible, the investigation will then be extended to a consideration of the effect of changing the surface tension, viscosity, and density of the liquids used for drop and target.

5. BIBLIOGRAPHY

1. Öpik, Ernst, Researches on the physical theory of meteor phenomena I, Toimetused Acta et Commentationes, Universitatis Tartuensis, XXX, [A] 4 (1936) (Tartu, Estonia).
2. Proceedings of the third symposium on hypervelocity impact, Vol. 1, Armour Research Foundation of Illinois Institute of Technology, Chicago, Ill. (Feb. 1959).
3. Cook, Melvin A., The science of high explosives (Reinhold Publishing Corporation, New York, N. Y., 1958).
4. Ungar, E. W., Investigation of high-speed particle erosion of melting aerodynamic surfaces, Final Report on Contract No. DA-33-019-ORD-2774, Battelle Memorial Institute, Columbus, Ohio (1959).
5. Worthington, A. M., On impact with a liquid surface, Proc. Roy. Soc. 34, 217 (1882).
6. Worthington, A. M., and Cole, R. S., Impact with a liquid surface, studied by the aid of instantaneous photography, Phil. Trans. Roy. Soc. 189A, 137 (1897).
7. Worthington, A. M., A study of splashes (Longmans, Green, and Company, New York, N. Y., 1908).
8. Edgerton, Harold E., and Killian, James R., Jr., Flash! Seeing the unseen by ultra high-speed photography (Charles T. Branford Company, Boston, 1954).
9. Franz, G. J., Splashes as sources of sound in liquids, J. Acous. Soc. Am. 31, 1080 (1959).
10. May, Albert, The influence of the proximity of tank walls on the water-entry behavior of models, NAVORD Report 2240, U. S. Naval Ordnance Laboratory, White Oak, Maryland, October 1951.
11. Partridge, William S., VanFleet, Howard B., and Whited, Charles R., An investigation of craters formed by high-velocity pellets, Technical Report No. OSR-9, Air Force Office of Scientific Research, May 1957.
12. Baldwin, Ralph B., The face of the moon (University of Chicago Press, Chicago, Ill., 1948).

USCOMM-NBS-DC

U. S. DEPARTMENT OF COMMERCE
Luther H. Hodges, *Secretary*

NATIONAL BUREAU OF STANDARDS
A. V. Astin, *Director*

THE NATIONAL BUREAU OF STANDARDS

The scope of activities of the National Bureau of Standards at its major laboratories in Washington, D.C., and Boulder, Colorado, is suggested in the following listing of the divisions and sections engaged in technical work. In general, each section carries out specialized research, development, and engineering in the field indicated by its title. A brief description of the activities, and of the resultant publications, appears on the inside of the front cover.

WASHINGTON, D.C.

Electricity. Resistance and Reactance. Electrochemistry. Electrical Instruments. Magnetic Measurements. Dielectrics.

Metrology. Photometry and Colorimetry. Refractometry. Photographic Research. Length. Engineering Metrology. Mass and Scale. Volumetry and Densimetry.

Heat. Temperature Physics. Heat Measurements. Cryogenic Physics. Equation of State. Statistical Physics.

Radiation Physics. X-ray. Radioactivity. Radiation Theory. High Energy Radiation. Radiological Equipment. Nucleonic Instrumentation. Neutron Physics.

Analytical and Inorganic Chemistry. Pure Substances. Spectrochemistry. Solution Chemistry. Analytical Chemistry. Inorganic Chemistry.

Mechanics. Sound. Pressure and Vacuum. Fluid Mechanics. Engineering Mechanics. Rheology. Combustion Controls.

Organic and Fibrous Materials. Rubber. Textiles. Paper. Leather. Testing and Specifications. Polymer Structure. Plastics. Dental Research.

Metallurgy. Thermal Metallurgy. Chemical Metallurgy. Mechanical Metallurgy. Corrosion. Metal Physics.

Mineral Products. Engineering Ceramics. Glass. Refractories. Enameled Metals. Crystal Growth. Physical Properties. Constitution and Microstructure.

Building Research. Structural Engineering. Fire Research. Mechanical Systems. Organic Building Materials. Codes and Safety Standards. Heat Transfer. Inorganic Building Materials.

Applied Mathematics. Numerical Analysis. Computation. Statistical Engineering. Mathematical Physics.

Data Processing Systems. Components and Techniques. Digital Circuitry. Digital Systems. Analog Systems. Applications Engineering.

Atomic Physics. Spectroscopy. Radiometry. Solid State Physics. Electron Physics. Atomic Physics.

Instrumentation. Engineering Electronics. Electron Devices. Electronic Instrumentation. Mechanical Instruments. Basic Instrumentation.

Physical Chemistry. Thermochemistry. Surface Chemistry. Organic Chemistry. Molecular Spectroscopy. Molecular Kinetics. Mass Spectrometry. Molecular Structure and Radiation Chemistry.

• Office of Weights and Measures.

BOULDER, COLO.

Cryogenic Engineering. Cryogenic Equipment. Cryogenic Processes. Properties of Materials. Gas Liquefaction.

Ionosphere Research and Propagation. Low Frequency and Very Low Frequency Research. Ionosphere Research. Prediction Services. Sun-Earth Relationships. Field Engineering. Radio Warning Services.

Radio Propagation Engineering. Data Reduction Instrumentation. Radio Noise. Tropospheric Measurements. Tropospheric Analysis. Propagation-Terrain Effects. Radio-Meteorology. Lower Atmosphere Physics.

Radio Standards. High Frequency Electrical Standards. Radio Broadcast Service. Radio and Microwave Materials. Atomic Frequency and Time Interval Standards. Electronic Calibration Center. Millimeter-Wave Research. Microwave Circuit Standards.

Radio Systems. High Frequency and Very High Frequency Research. Modulation Research. Antenna Research. Navigation Systems. Space Telecommunications.

Upper Atmosphere and Space Physics. Upper Atmosphere and Plasma Physics. Ionosphere and Exosphere Scatter. Airglow and Aurora. Ionospheric Radio Astronomy.


NBS